

Improving resolution of gravity data with wavelet analysis and spectral method

QIU Ning^{1,3}, HE Zhanxiang², CHANG Yanjun (✉)^{1,3}

- 1 Institute of Geophysics and Geomatics, China University of Geosciences, Wuhan 430074, China
2 Geophysical Prospecting Bureau, China National Petroleum Corporation, Zhuozhou 072751, China
3 Open Laboratory of Engineering Geophysics, Ministry of Land and Resources, Wuhan 430074, China

© Higher Education Press and Springer-Verlag 2007

Abstract Gravity data are the results of gravity force field interaction from all the underground sources. The objects of detection are always submerged in the background field, and thus one of the crucial problems for gravity data interpretation is how to improve the resolution of observed information. The wavelet transform operator has recently been introduced into the domain fields both as a filter and as a powerful source analysis tool. This paper studied the effects of improving resolution of gravity data with wavelet analysis and spectral method, and revealed the geometric characteristics of density heterogeneities described by simple shaped sources. First, the basic theory of the multiscale wavelet analysis and its lifting scheme and spectral method were introduced. With the experimental study on forward simulation of anomalies given by the superposition of six objects and measured data in Songliao plain, Northeast China, the shape, size and depth of the buried objects were estimated in the study. Also, the results were compared with those obtained by conventional techniques, which demonstrated that this method greatly improves the resolution of gravity anomalies.

Keywords gravity anomalies, spectral analysis, Songliao plain, wavelet

1 Introduction

One of the most common problems encountered in geophysical studies is how to improve the resolution of observed information. In this paper, great effort has been given to solve this problem by combining the wavelet analysis and the spectral method. To better understand the specific characteristics of

our approach, first, the existing techniques and their significance in establishing modern investigation methods in the potential fields were reviewed. Several techniques are concerned about transforming the measured field and source characterization. Empirical graphical procedures were first proposed. They show reasonable determination of the depth to magnetization distributions of defined shapes (Peters, 1949). Then, another method was devoted to comparing an observed field with analytic models—first, by means of charts (Chastenot de Gery and Naudy, 1957), and later by a variety of different techniques that use synthetic model fitting, such as Werner deconvolution (Werner, 1953), automated by Ku and Sharp (1983), Euler deconvolution (Thompson, 1982), and analytic signal (Nabighian, 1972, 1974). A lot of applications and improvements of these methods have been tried, such as the use of vertical gradients (Marson and Klingele, 1993) and considering the effect of noise in data (Keating, 1998). These techniques have always been used on the basis of assuming a chosen geometry of the source. Stavrev (1997) investigated the revelation of both shape and depth of sources using methods derived from the Euler deconvolution and the analytic signal technique (Hsu et al., 1998). Fourier analysis has triggered a wide range of applications in the potential-fields, both for data filtering (Bhattacharyya, 1972) and transforming and for sources characterization (Blakely, 1995). The wavelet transform has been developed as a powerful analysis tool (Holschneider, 1995) and has been introduced into the geophysical field (Foufoula-Georgiou and Kumar, 1994). The purposes of both Fourier and wavelet operators are to investigate the behavior of the measured field in terms of wavelengths. The Fourier technique is more efficient in estimating depth information than estimating stationary undulating surfaces (Spector and Grant, 1970), while its application may become a problem when the signal is not stationary. The use of the wavelet operator instead, as first defined by Grossman and Morlet (1984), allows wavelength-adaptive convolution operators to vary the wavelength of the studied portion of

Translated from *Progress in Geophysics*, 2007, 22(1): 112–120 [译自: 地球物理学进展]

E-mail: Changyj@cug.edu.cn

signal. In other words, the wavelet operator can focus on individual object. The special class of wavelets used in this study can analyze the scaling properties of the source via upward continuation. A general n -dimensional theoretical framework for local homogeneous sources has been developed by Moreau et al. (1997, 1999). With this approach, Sailhac et al. (2000) addressed the issue of the magnetic anomalies interpretation.

Recently, Martelet et al. (2001) used 1-D wavelet transform on gravity data to characterize geological boundaries. Fedi et al. (2004) proposed the combined application of continuous and discrete wavelet transform to identify shallow and deep sources on gravity data. Ning et al. (2005) applied the multiscale edge constraint to enhance the stability of downward continuation. The depth from extreme points (DEXP) method is proposed to determine the depth and the structural index of potential field sources (Fedi, 2007). The wavelet analysis has been applied to analyze the coherence between Bouguer gravity and topography of the elastic thickness anisotropy in the Canadian Shield (Audet and Mareschal, 2007). Here, we discussed the technique capabilities for gravity data by combining wavelet with power spectrum analysis, which estimates the shape, size and depth of the buried objects. Then, its results were compared with those obtained by conventional techniques.

2 Background of the methods

2.1 Multiscale wavelet analysis

Gravity data observed in geophysical surveys are the sum of gravity fields produced by all underground sources. The targets for specific surveys are often small-scale structure, buried at shallow depths, and are embedded in a regional field arising from residual sources, which are usually larger, deeper than, or located far from the targets. Correct estimation and removal of the regional field from initial field observations yield the residual field produced by the target sources. Interpretation and numerical simulation are carried out on the residual field data, and the reliability of the interpretation depends upon the success of the regional-residual separation to a great extent.

The Grossmann and Morlet's (1984) definition of the continuous wavelet transform for a 1-D signal $f(x) \in L^2(R)$ with respect to the analyzed wavelet $\psi(x) \in L^2(R)$ is

$$\begin{aligned} W(a,b) &= k(a) \int_{-\infty}^{\infty} f(x) \bar{\psi} \left(\frac{y-x}{a} \right) dx \\ &= k(a) \int_{-\infty}^{\infty} f(x) \tilde{\psi} \left(\frac{x-b}{a} \right) dx, \end{aligned} \quad (1)$$

where $\tilde{\psi}(x) = \bar{\psi}(x)$; $a \in R^+$ and $b \in R$, are the scale and the position parameters, respectively, with R^+ being the set of positive real numbers; $L^2(R)$ denotes the Hilbert space of square integrable functions, and the bar denotes the conjugated complex. The constant $k(a)$ can be taken to $1/\sqrt{R}$

in order to insure normalization in energy of the set of wavelets $\psi \left(\frac{x-b}{a} \right)$ obtained by a translation and dilation of the "mother wavelet" ψ . Discrete families of orthonormal wavelets

$$\psi_{L,k}(x) = \frac{1}{\sqrt{2^l}} \psi \left(\frac{x-k2^l}{2^l} \right) = \frac{1}{\sqrt{2^l}} \psi(2^{-l}x - k) \quad (2)$$

are obtained by dilating or contracting and translating $\psi_{0,0}$, with the choice $a = 2^l$ and $b = ka$ with $l, k \in Z$ (Z is the set of integers).

In this case, the discrete wavelet transform (DWT) is

$$\tilde{w}_{L,k}(x) = \int_{-\infty}^{\infty} f(x) \psi_{l,k}(x) dx \quad (3)$$

and the inverse discrete wavelet transform in the L^2 -sense (IDWT) is

$$f(x) = \sum_{l=-\infty}^{+\infty} \sum_{k=-\infty}^{+\infty} \tilde{w}_{l,k} \psi_{l,k}(x) \quad (4)$$

The advantage of analyzing a signal with wavelets is that it enables the study on local features of the signal with a detailed matching to their characteristic scale. In the temporal domain such a property allows for an effective representation of transient signals. Because a major potential application of wavelets is image processing, 2-D DWT is necessary. Let t_1 and t_2 be the 2-D coordinates, and then the 2-D separable scaling function is

$$\phi^{(1)}(x, y) = \phi(x)\psi(y) \quad (5)$$

Original signal can be reconstructed. Then 2-D separable wavelets are

$$\psi^{(1)}(x, y) = \phi(x)\psi(y) \quad (6)$$

$$\psi^{(2)}(x, y) = \psi(x)\phi(y) \quad (7)$$

$$\psi^{(3)}(x, y) = \phi(x)\phi(y) \quad (8)$$

In scale $j + 1$, separable approximation

$$f_{2^{j+1}}^0(m, n) = \langle f_{2^j}^0(x, y), \phi(x - 2m), y - 2n \rangle \quad (9)$$

In scale $j + 1$, separable detail at horizontal, vertical, diagonal directions

$$f_{2^{j+1}}^1(m, n) = \langle f_{2^j}^0(x, y), \psi^1(x - 2m), y - 2n \rangle \quad (10)$$

$$f_{2^{j+1}}^2(m, n) = \langle f_{2^j}^0(x, y), \psi^2(x - 2m), y - 2n \rangle \quad (11)$$

$$f_{2^{j+1}}^3(m, n) = \langle f_{2^j}^0(x, y), \psi^3(x - 2m), y - 2n \rangle \quad (12)$$

Because wavelet analyses do not decompose signals into sines and cosines, a purely periodic signal of frequency F_p

(pseudofrequency) is defined to allow wavelet decomposition of the signals to be related to the more traditional Fourier decomposition. This is a convenient way of characterizing the dominant frequency of the wavelet (Abry, 1997) and its application in bioscience (Karlsson et al., 2000) and in geosciences (Zhou and Adeli, 2003). Pseudofrequency corresponding to the scale of wavelet decomposition is calculated as

$$F_p = \frac{F_w \cdot \Delta}{a} \tag{13}$$

where a is a scale, Δ is the sampling period, and F_w is the center frequency of the wavelet in Hz (i.e. the frequency corresponding to the spectral peak of the wavelet). The sampling period Δ and the scale a take into account dilations and contractions of the wavelet function.

Recently, a method for implementing lifting-based DWT has been proposed (Sweldens, 1995; Daubechies and Sweldens, 1998) and applied (Jiang and Ortega, 2001; Andra et al., 2002; Xiong et al., 2004) because the lifting-based DWT has many advantages over the convolution-based one. The lifting scheme is a new method based on spatial to construct wavelet, which comprises three steps: splitting, predicting, and update lifting, as well as scale normalization. Lifting wavelet (Sweldens, 1995) is called the second generation wavelet, the basic principle of which is to break up the polyphase matrices for the wavelet filters into a sequence of upper and lower triangular matrices and convert the filter implementation into banded matrix multiplications.

2.2 Spectral estimation of depth

The depth extent of gravity sources can be of considerable geologic interest. Two types of methods have been commonly used in the spectral estimation of the depth to the bottom of the layer (Ravat et al., 2007): (1) the spectral peak method originally proposed in a landmark paper by Spector and Grant (1970) and then used by Shuey et al. (1977), Connard et al. (1983) and Blakely (1988); and (2) the centroid method originally presented by Bhattacharyya and Leu (1977) and used with certain caveats and variations by Okubo et al. (1985) and Tanaka et al. (1999).

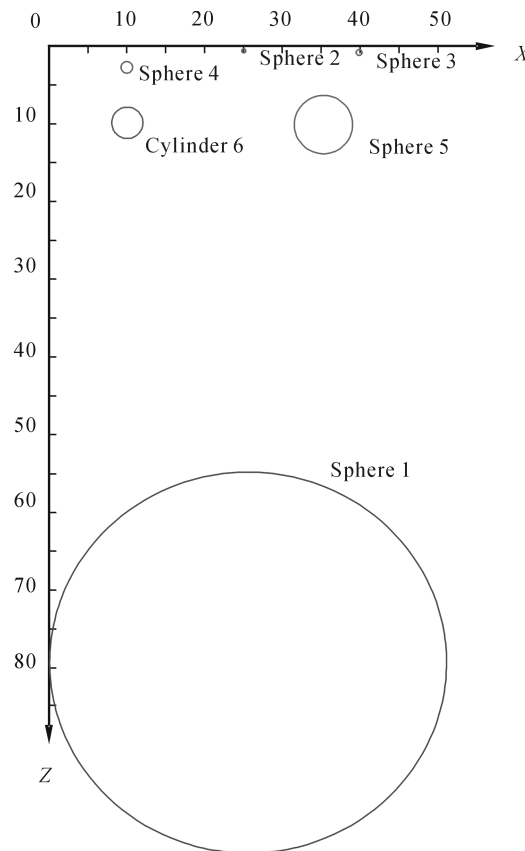


Fig. 1 Cut-open view of synthetic gravity anomaly sources
 Note: grid size is 50 km × 50 km, sampling interval is 0.25 km.
 For the shape, coordinate, size and density of these objects, see Table 1

The spectral factorization method (Spector and Grant, 1970) is based on the assumption that interfaces are essentially horizontal with some small relief. The gravitational variation of this subsurface topography can be described in the frequency domain by the first term of Parker’s expansion (Parker, 1972). Assuming a group of prismatic sources distributed over the subsurface topography, the gravity Fourier power spectrum of the group of bodies reveals a quasilinear relationship between the wavenumber and the Fourier power spectral density. Plotting the natural logarithm of the radially

Table 1 Parameter of the shape, coordinate, size and density of synthetic gravity anomaly sources

Objects No.	1	2	3	4	5	6
Shape	Sphere	Sphere	Sphere	Sphere	Sphere	Cylinder
x, y, z coordinate/km	25, 25, 80	25, 25, 0.6	40, 20, 1	10, 40, 3	35, 35, 12	10, 0–50, 12
Radius/km	25	0.4	0.5	1	4	2
Density/($g \cdot m^{-3}$)	1.8	1.0	1.0	1.0	1.6	1.2

Table 2 Parameter of wavenumber, wavelength and scale corresponding to detail and approximation at each levels using wavelet separate respectively

Levels	Detail at first	Detail at second	Detail at third	Detail at fourth	Detail at 51st	Detail at sixth	Approx. at sixth
Scale	2	4	8	16	32	64	64
Wave number scope at x, y directions	1.294–0.647	0.647–0.324	0.324–0.162	0.161–0.081	0.081–0.041	0.041–0.021	≤ 0.021
Wave length scope at x, y directions	0.773–1.545	1.545–3.090	3.090–6.180	6.180–12.361	12.361–24.722	24.722–49.443	≥ 49.443

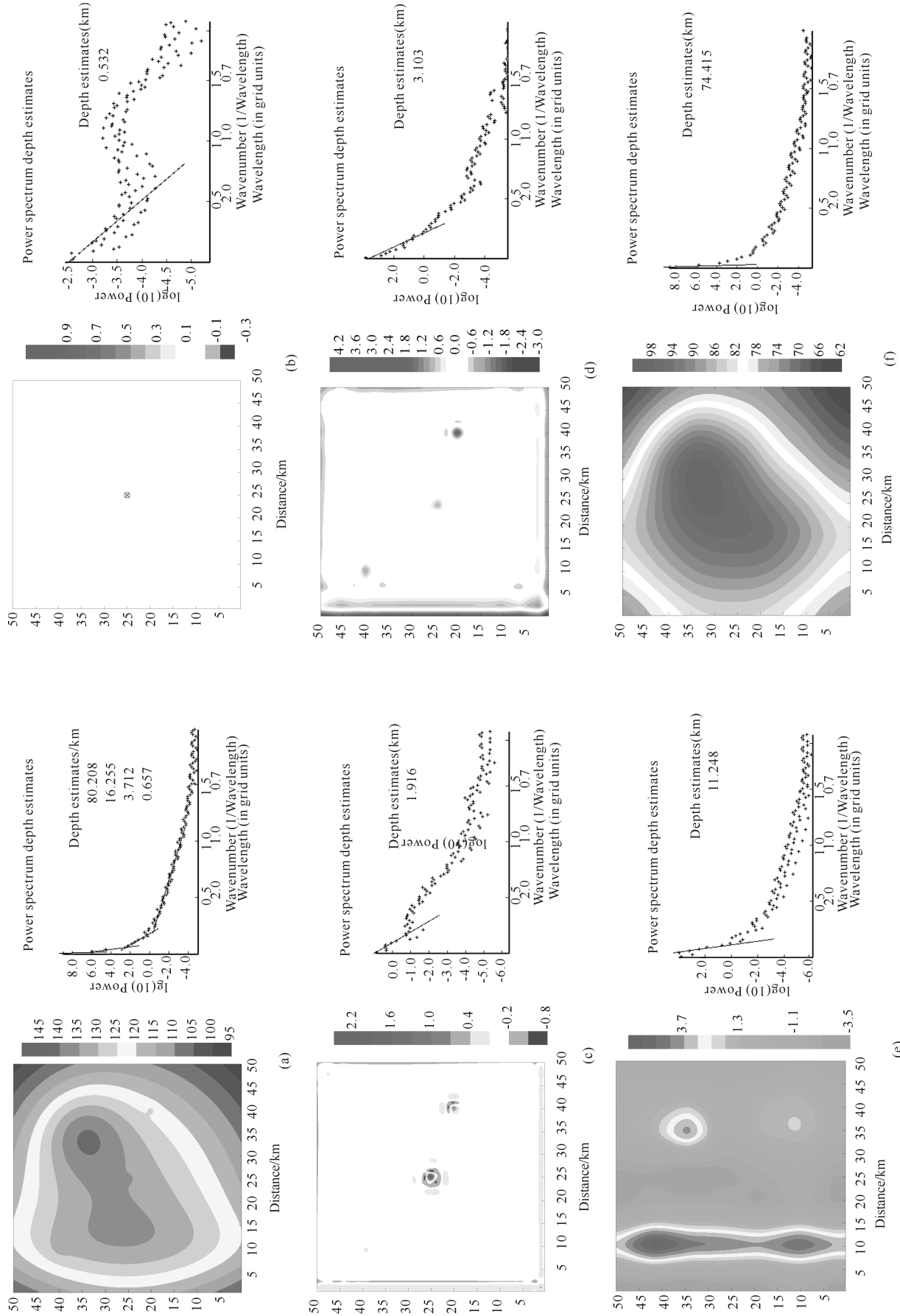


Fig. 2 Results of synthetic gravity anomaly data applied by wavelet and spectral analysis at six levels respectively (a) Synthetic anomaly data; (b) Detail at first level; (c) Detail at third level; (d) Detail at fourth level; (e) Approximation at sixth level

averaged Fourier power spectrum of the free-air anomaly versus wavenumber results in several lines, which correspond to the mean depths of the density contrast. The power spectrum of the gravity is anomaly in relation to the average depth of the disturbing interface

$$P_k = \left(\sum_{j=0}^{n-1} g(x_j, z) e^{-i2\pi kx_j} e^{2\pi kz} \right)^2 \tag{14}$$

where $g(x_j, z)$ is an anomaly with n data points in z depth, wavenumber k is defined therefore as the amplitude $k=1/\lambda$. Plotting wavenumber k against $\log_e P_k$ to attain the average depth to the disturbing interface. The interpretation of the against wavenumber k requires the best fit line through the lowest wavenumbers of the spectrum. The average depth can be estimated from plotting the spectrum.

$$\bar{h} = \frac{\Delta P}{4\pi\Delta k} \tag{15}$$

where \bar{h} is the average depth, and ΔP and Δk are derivatives of P and k , respectively.

3 Experimental study

3.1 Synthetic anomalies

Forward simulation anomalies given by the superposition of six objects are considered, which correspond respectively to five shallower structures and to a deeper one, each distributed in a 3-dimensional space.

In Cartesian coordination, the gravitational potential is denoted by U , the vertical attraction of gravity measured by the gravity meters (Blakely, 1995) is

$$g(x, y, z) = \frac{\partial U}{\partial z} = \iiint_{z' y' x'} \rho(x', y', z') \psi(x-x', y-y', z-z') dx' dy' dz' \tag{16}$$

where

$$\psi(x, y, z) = -\gamma \frac{z}{(x^2 + y^2 + z^2)^{3/2}}$$

The forward method requires the repeated calculation using Eq. (16). Table 1 shows the shape, coordinate, size and density of these objects. In this synthetic data, grid size is 50 km × 50 km and sampling interval is 0.25 km. While region field shows the effect of the deepest object, local field shows the effect of five shallow objects. Figure 1 shows the depth drawing the cut-open view of synthetic gravity sources.

The data were decomposed into six levels by applying a type of wavelet, possessed to be symmetry, compact supported, smooth, and biorthogonal. Table 2 shows the correspondent relationship between wavenumber and wavelength. The scale of detail and approximation at each level can be obtained using Eq. (13). Figure 2 shows the result of synthetic gravity anomaly data by applying wavelet and spectral analysis at six levels. It is shown in Fig. 2(b) that the detail displays a cone-like structure corresponding to object No. 2, which is the shallowest structure equivalent to 0.6 km in depth. In Fig. 2(c), detail shows another cone-like structure corresponding to object No. 3, which is the second shallowest structure equivalent to 1 km in depth. In Fig. 2(d), the detail shows a structure corresponding to object No. 4, which is a shallow structure equivalent to 3 km in depth. In Fig. 2(e), the detail shows a cone-like structure and a strip-like one corresponding to object No. 5 and No. 6, which is the second deeper structure equivalent to 12 km in depth. Finally, in Fig. 2(f), the detail shows a larger structure corresponding to object No. 1, which is the deepest structure equivalent to 80 km in depth.

For the purpose of comparison, the synthetic data were analyzed with the conventional method discussed above. Figure 3(a) shows the second derivative of synthetic gravity anomaly. Figure 3(b) and (c) show the result of synthetic data after moving 300 times iterated. In comparison with the result

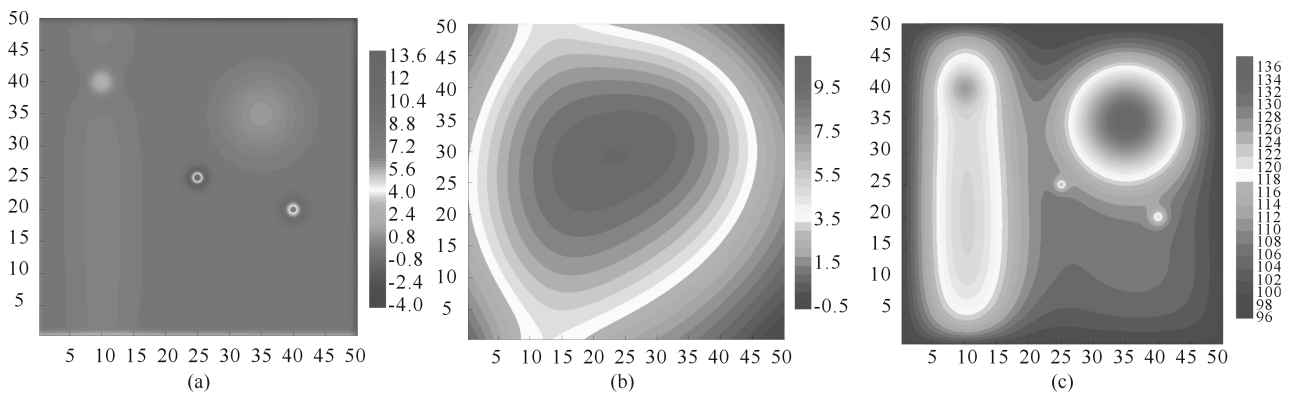


Fig. 3 Result of synthetic gravity anomaly data processed by conventional method

Note: (a) shows the second derivative of synthetic data; (b) and (c) show the result of synthetic data applied by moving average method after 300 times iterated.

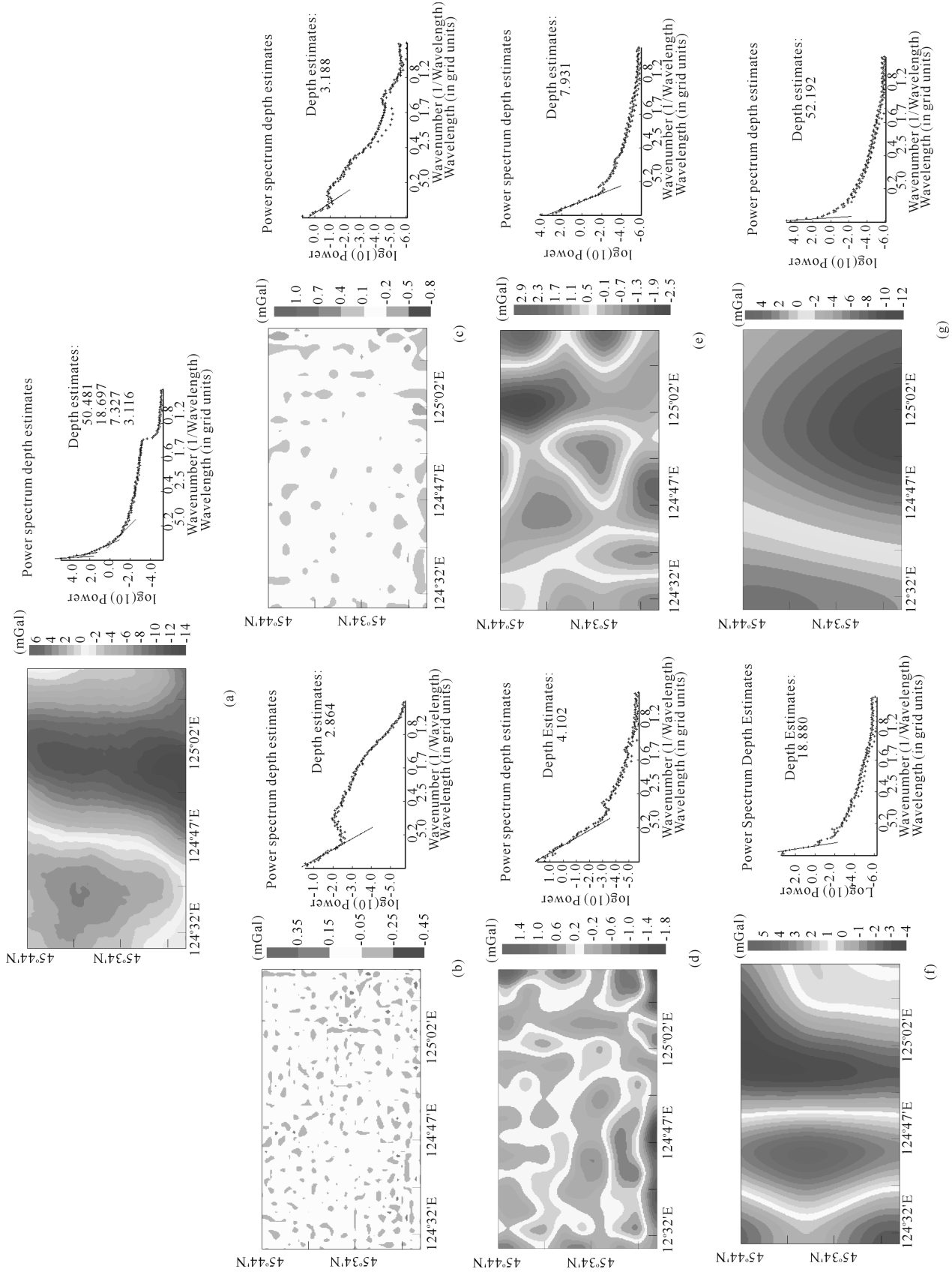


Fig. 4 Result of measured data in Songliao plain, northeast of China, applied by wavelet and spectral analysis at five levels (a) Measured gravity anomalies; (b) Detail at first level; (c) Detail at second level; (d) Detail at third level; (e) Detail at fourth level; (f) Detail at fifth level; (g) Approximation at fifth level

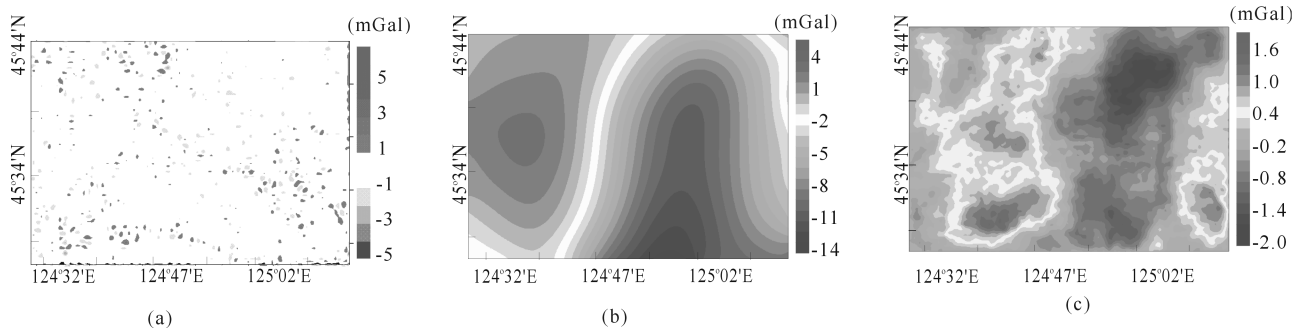


Fig. 5 Result of measured data in Songliao plain, Northeast China, processed by conventional method

Note: (a) shows the second derivative of measured data; (b) and (c) show the result of measured data applied by moving average method after 300 times iterated

of the multiscale wavelet and spectral method, the results of these conventional techniques have no improving resolution ability to easily distinguish the local field from the region field without a priori estimation of the layer. Moreover, it is convenient to determine the depth corresponding to the structure by the multiscale wavelet and spectral method.

3.2 Measured data in Songliao

Twenty four gravity measurements along a north-south profile were collected. Figure 4(a) shows measured gravity anomalies of Songliao plain in Northeast China. Figure 4(b)–(g) show the result of measured data applying wavelet and spectral analysis at five levels.

Similarly, to compare this method with conventional techniques, the measured data were possessed by smoothing method. Figure 5(a) shows the second derivative of measured data. Despite in rough correspondence to the detail at first (see Fig. 4(b)) and third levels (see level Fig. 4(d)) decomposed by wavelet, the results are not as good as those decomposed by the wavelet. The residue field was rough, corresponding to the approximation at fifth level, and the region field was also rough, corresponding to the detail at fourth and fifth levels, which fairly fitted the observed structures.

4 Conclusions

Geophysical gravity field interpretation constantly suffers from the well-known nonuniqueness of the inversion, and thus needs additional priori information. Several existing methods have been proposed to analyze the gravity field prior to modeling to extract useful information. The technique described in this paper combines the upward continuation, derivation operators and spectral analysis into a new convenient formalism.

It has shown that this wavelet and spectral method allows deep sources when the corresponding gravity anomalies merged with anomalies of sources at shallow depths. This is a special case of multisource problem, which frequently occurs in potential field interpretation. The wavelet analysis

is necessary for separating the shallow-source anomalies from the deep-source ones, benefiting also from the optimum shift criterion and the well-known properties of localized filtering of this kind of wavelet transform (Fedi and Quarta, 1998). Although the separation of gravity fields is always a very tricky task, we showed the experimental results of forward simulation and measured data cases where the superpositions of deep objects are fairly well-separated. Moreover, the spectral estimation of the separated detail can roughly gain the depth in rough correspondence to structures, which has contributed to the resolution for data interpretation.

Acknowledgements We thank Liu Yunxiang, Ji Liansheng, Song Jingming and Liu Xuejun from Bureau of Geophysical Prospecting, China National Petroleum Corporation (BGP, CNPC) for fruitful discussions. All data were acquired under the support from BGP. We also thank anonymous reviewers and editors for valuable comments that improved the manuscript. This work was supported by the Science Research and Technology Development Program of CNPC (No. 04B020500) and the Hubei Province Natural Science Foundation of China (No. 2005ABA275).

References

- Abry P (1997). Ondelettes et turbulence, Multirésolutions, Algorithmes de Décomposition. Paris: Invariance D'échelles
- Andra K, Chakrabarti C, Acharya T (2002). A VLSI architecture for lifting-based forward and inverse wavelet transform. *IEEE Transactions on Signal Processing*, 50(4): 966–977
- Audet P, Mareschal J C (2007). Wavelet analysis of the coherence between Bouguer gravity and topography: Application to the elastic thickness anisotropy in the Canadian Shield. *Geophysical Journal International*, 168(1): 287–298
- Bhattacharyya B K (1972). Design of spatial filters and their application to high-resolution aeromagnetic data. *Geophysics*, 37(1): 68–91
- Bhattacharyya B K, Leu L K (1977). Spectral analysis of gravity and magnetic anomalies due to rectangular prismatic bodies. *Geophysics*, 42(1): 41–50
- Blakely R J (1988). Curie temperature isotherm analysis and tectonic implications of aeromagnetic data from Nevada. *Journal of Geophysical Research*, 93(B10): 11817–11832
- Blakely R J (1995). *Potential Theory in Gravity and Magnetic Applications*. Cambridge: Cambridge University Press
- Chastenot de Gery J, Naudy H (1957). Sur l'interprétation des anomalies gravimétriques et magnétiques. *Geophysical Prospecting*, 5(4): 421–448

- Connard G, Couch R, Gemperle M (1983). Analysis of aeromagnetic measurements from the Cascade Range in central Orogen. *Geophysics*, 48(3): 376–390
- Daubechies I, Sweldens W (1998). Factoring wavelet transforms into lifting steps. *Journal of Fourier Analysis and Its Applications*, 4(3): 247–269
- Fedi M (2007). DEXP: A fast method to determine the depth and the structural index of potential fields sources. *Geophysics*, 72(1): 11–111
- Fedi M, Primiceri R, Quarta T, et al (2004). Joint application of continuous and discrete wavelet transform on gravity data to identify shallow and deep sources. *Geophysical Journal International*, 156(1): 7–21
- Fedi M, Quarta T (1998). Wavelet analysis for the regional-residual and local separation of the potential field anomalies. *Geophysical Prospecting*, 46(5): 507–525
- Foufoula-Georgiou E, Kumar P (1994). *Wavelets in Geophysics*. San Diego: Academic Press, 1–43
- Grossman A, Morlet J (1984). Decomposition of hardy functions into square integrable wavelets of constant shape. *Journal on Mathematical Analysis*, 15(4): 723–736
- Holschneider M (1995). *Wavelets: An Analysis Tool*. New York: Oxford University Press
- Hsu S K, Coppens D, Shyu C T (1998). Depth to magnetic source using the generalized analytic signal. *Geophysics*, 63(6): 1947–1957
- Jiang W, Ortega A (2001). Lifting factorization-based discrete wavelet transform architecture design. *IEEE Transaction on Circuits and Systems for Video Technology*, 11(5): 651–657
- Karlsson S, Yu J, Akay M (2000). Time-frequency analysis of myoelectric signals during dynamic contractions: A comparative study. *IEEE Transactions on Biomedical Engineering*, 47(2): 228–238
- Keating P B (1998). Weighted Euler deconvolution of gravity data. *Geophysics*, 63(5): 1595–1603
- Ku C C, Sharp J A (1983). Werner deconvolution for automated magnetic interpretation and its refinement using Marquardt's inversed modeling. *Geophysics*, 48(6): 754–774
- Marson I, Klingele E E (1993). Advantages of using the vertical gradient of gravity for 3-D interpretation. *Geophysics*, 58(11): 1588–1595
- Martelet G, Sailhac P, Moreau F, et al (2001). Characterization of geological boundaries using 1-D wavelet transform on gravity data: Theory and application to the Himalayas. *Geophysics*, 66(4): 1116–1129
- Moreau F, Gibert D, Holschneider M, et al (1997). Wavelet analysis of potential fields. *Inverse Problems*, 13(3): 165–178
- Moreau F, Gibert D, Holschneider M, et al (1999). Identification of sources of potential fields with the continuous wavelet transform: Basic theory. *Journal of Geophysical Research*, 104(B3): 5003–5013
- Nabighian M N (1974). Additional comments on the analytic signal of two-dimensional magnetic bodies with polygonal cross-section. *Geophysics*, 39(1): 85–92
- Nabighian N N (1972). The analytic signal of two-dimensional magnetic bodies with polygonal cross-section. *Geophysics*, 37(2): 507–517
- Ning J S, Wang H H, Luo Z C (2005). Downward continuation of gravity signals based on the multiscale edge constraint. *Chinese Journal of Geophysics*, 48(1): 63–68 (in Chinese with English abstract)
- Okubo Y, Graf R J, Hansen R O, et al (1985). Curie point depths of the Island of Kyushu and surrounding areas, Japan. *Geophysics*, 50(3): 481–494
- Parker R L (1972). The rapid calculations of potential anomalies. *Geophysical Journal International*, 31(4): 447–455
- Peters L J (1949). The direct approach to magnetic interpretation and its practical application. *Geophysics*, 14(3): 290–320
- Ravat D, Pignatelli A, Nicolosi I, et al (2007). A study of spectral methods of estimating the depth to the bottom of magnetic sources from near-surface magnetic anomaly data. *Geophysical Journal International*, 169(2): 421–434
- Sailhac P, Galdeano A, Gibert D, et al (2000). Identification of sources of potential fields with the continuous wavelet transform: Complex wavelets and application to aeromagnetic profiles in French Guiana. *Journal of Geophysical Research*, 105(B8): 19455–19475
- Shuey R T, Schellinger D K, Tripp A C, et al (1977). Curie depth determination from aeromagnetic spectra. *Geophysical Journal of the Royal Astronomical Society*, 50: 75–101
- Spector A, Grant F S (1970). Statistical models for interpreting aeromagnetic data. *Geophysics*, 35(2): 293–302
- Stavrev P Y (1997). Euler deconvolution using differential similarity transformations of gravity or magnetic anomalies. *Geophysical Prospecting*, 45(2): 207–246
- Sweldens W (1995). The lifting scheme: A new philosophy in biorthogonal wavelet constructions. In: Laine A F, Unser M, ed. *Wavelet Applications in Signal and Image Processing III*. Proceedings of SPIE—The International Society for Optical Engineering. Society of Photo-Optical Instrumentation Engineers, San Diego, CA, USA, 68–79
- Tanaka A, Okubo Y, Matsubayashi O (1999). Curie point depth based on spectrum analysis of the magnetic anomaly data in East and Southeast Asia. *Tectonophysics*, 306(3–4): 461–470
- Thompson D T (1982). A new technique for making computer-assisted depth estimates from magnetic data. *Geophysics*, 47(1): 31–37
- Werner S (1953). Interpretation of magnetic anomalies of sheet-like bodies. *Sveriges Geologiska Undersökning Arsbok*, 43(6): 508
- Xiong C, Tian J, Liu J (2004). A fast VLSI architecture for two-dimensional discrete wavelet transform based on lifting scheme. *Proceedings Seventh International Conference on Solid-State and Integrated Circuits Technology*, 1661–1664
- Zhou Z, Adeli H (2003). Time-frequency signal analysis of earthquake records using Mexican Hat wavelets. *Computer-Aided Civil and Infrastructure Engineering*, 18(5): 379–389